Conjugation to gold nanoparticles improves antigen immunogenicity

A. E. Gregory [1*], E. D. Williamson[2], J. L. Prior [2], W. Butcher [2], I. J. Thompson[2], A. M. Shaw [1], R. W. Titball [1]

[1] *School of Biosciences, University of Exeter, Devon, EX4 4QD, UK*;
[2] *Defence Science and Technology Laboratory, Porton Down, SP4 0JQ, UK*

* corresponding author:
e-mail: anthony.gregory@exeter.ac.uk
Tel; 01392 725177

Key words; *Plague, Y. pestis, gold nanoparticle, vaccine, carbodiimide*

Running title; gold nanoparticle vaccine

Abstract

The effectiveness efficacy of a gold nanoparticle delivery system for the the rF1 plague antigen was assessed by immunising mice with a coupled vaccine formulation. In this study, we describe a method for conjugating a capsular protein (F1-antigen) from *Yersinia pestis* onto gold nanoparticles as a potential delivery vehicle for subunit vaccines. The gold nanoparticles used in the experiment were 15 nm citrate-reduced particles and were decorated with the antigen using *N*-hydroxysuccinimide and 1-ethyl-3-(3-dimethylaminopropyl) carbodiimide coupling chemistry and characterised. The immunogenicity was assessed in BALB/c mice showing that F1-antigen conjugated 15 nm gold nanoparticles produced an enhanced specific IgG response compared with the unconjugated nanoparticle control, The IgG-specific antibody titre was further elevated when the F1-functionalised nanoparticles were co-administered with an alhydrogel adjuvant. The antisera raised competiatively displaced antibodies from an rF1 previously identified protective Macaque serum?. When delived in in PBS without an adjuvant, the F1 conjugated gold nanoparticles induced a significantly increased IgG2a response compared with unconjugated F1 in PBS ($p<0.05$). The conjugation of F1 to gold nanoparticles altered the IgG1: IgG2a ratio from 14.04 for F1/PBS to 6.72 for F1 conjugated to gold nanoparticles and administered in PBS ($p<0.01$). All treatment groups developed a cellular memory response to F1, the polarity of which was inflenced by formulation in alhydrogel.

Introduction

Yersinia pestis is a Gram-negative, facultative intracellular bacterium belonging to the enterobacteriacae – should this be in italic? family. It is the causative agent of plague which, throughout history, has killed over 200 million people worldwide (1). There is currently no vaccine against plague and the isolation of multi-drug resistant strains as well as the concern for its use in bioterrorism has led to resurgence in *Y. pestis* research in recent years.???

The field of nanotechnology has, in recent years, expanded with growing applicability to medical biotechnology. One area of interest includes the use of nanoparticles (NPs) in drug delivery. Since they were first proposed in the 1970's, liposome's have been studied for their use in drug encapsulation. Ordinarily composed of amphiphilic phospholipids and cholesterol, liposome's self-associate to form spherical micelles, typically 400 nm in diameter, with an aqueous interior (2). Using a variety of methods, this process can be manipulated to encapsulate drugs within the aqueous interior offering a route of delivery for water-insoluble drugs. There are however some limitations associated with liposomes such as weak stability, poor drug loading, toxicity and polydispersal (3-5). To overcome some of these restrictions, people have turned to polymeric micelles which can be made from inert materials or biodegradable polymers such as poly-L-lactide (PLA) or poly-L-lactide-co-glycolides (PLGA). In much the same way, these formulations offer drug encapsulation within a hydrophobic core as well as a hydrophilic shell to which polar molecules can absorb. Traditionally a solvent is used to improve solubility of water-insoluble drugs however this is often toxic and will limit the dose at which the drug can be given. An example of such a drug where nanoencapsulation has overcome this problem is the Food and Drug Administration (FDA)-approved Abraxane; an albumin bound NP formulation of paclitaxel (6). A mitotic inhibitor drug, it is given to treat breast cancer although due to its poor solubility, it was previously dissolved in Cremophor EL for administration. Nanoencapsulation is also a very important tool for protection of a transported antigen, particularly if it is susceptible to degradation, such as DNA.

Solid NPs have also been explored for their use in drug delivery, ranging from cadmium to chitosan and encompassing all sizes from 1-100 nm. Much of the work in this field has focused onto site directed drug delivery, which has been most useful in cancer therapy where it is paramount to distinguish between cancerous and normal cells. One way in which this has been demonstrated is by taking advantage of the impaired lymphatic recovery system associated with tumours. By conjugating a NP copolymer of styrene and maleic acid to the antitumor protein neocarzinostatin, the authors were able to demonstrate that NPs of 10-100 nm avoid uptake by the reticuloendothelial system and accumulate within tumours (7). Another type of targeted delivery using NPs uses the unique optical properties of metals on a nano-scale which often behave differently to that on a macro-scale. Gold, for example, has become a very popular choice for nano-medicine (refs). It has a high atomic number allowing for *in vivo* electron microscope and X-ray imaging – what does that mean? but also its surface plasmon resonance will absorb light at a specific wavelength and convert it to heat. This too has been used in cancer therapy where a cancer-specific antibody has been conjugated onto 20 nm gold NPs (AuNPs) and then irradiated with

a low power laser at the site of interest to destroy the tumour cells (8). Despite the exciting possibilities NPs offer to medicine, one should not forget the safety issues associated with such materials. Indeed some, including TiO_2 and Cu_2O, have demonstrated harmful effects in terms of tissue damage due to reactive oxygen species and accumulation within cells (9-12).

Herein we describe a method for conjugating a previously identified vaccine candidate against *Y. pestis*, capsular protein (F1-antigen) [10], onto citrate reduced AuNPs (13), to test whether the presentation of the antigen on the AuNP surface area will encourage opsonisation and therefore improve immunogenicity.

2. Materials and methods

2.1 Nanoparticle synthesis
Gold(III) chloride trihydrate ($HAuCl_4 \cdot 3H_2O$, 99.9%), sodium citrate dihydrate ($C_6H_5O_7 \cdot 2H_2O$, 99%), *N*-(3-dimethylaminopropyl)-*N'*-ethylcarbodiimide hydrochloride (EDC) and *N*-hydroxysuccinimide (NHS, 98%) were purchased from Sigma-Aldrich Co. Ltd. (Gillingham, UK).

AuNPs were synthesised using the Turkevich method (14). Briefly, all glassware used was first washed in *aqua regia* (three parts concentrated HCl to one part of concentrated HNO_3) before heating 90 ml 1mM $HAuCl_4.3H_2O$ to $90^{\circ}C$ whilst stirring vigorously. Next, 10 ml 90 mM $Na_3C_6H_5O_7$ was quickly added to the gold solution before cooling to room temperature in the dark. Characterisation of the particles was carried out using Ultraviolet-Visible spectroscopy and their diameter determined by transmission electron microscopy (TEM), yielding a mean value of 15.6 nm.

2.2 Conjugation of protein onto gold nanoparticles
Recombinant F1-antigen (rF1) was immobilised onto the gold spheres using carbodiimide chemistry. To a NP solution, 0.1 mM 16-mercaptohexadecanoic acid (MHDA) was added followed by 0.1% (vol/vol) Triton®-x 100 and left to incubate for two hours at room temperature. To purify the carboxylated nanospheres, the sample was centrifuged at 13,000 x g for 10 min after which the supernatant was removed and the pellet re-suspended in phosphate buffered saline (PBS). N-hydroxysuccinimide (NHS) and 1-ethyl-3-(3-dimethylaminopropyl) carbodiimide (EDC), 0.15 mM and 0.6 mM respectively, was then added to the functionalised NPs before adding 20 μg/ml rF1. The solution was left to incubate at room temperature for 2 h. Later, this was centrifuged as before to isolate the conjugated NPs which were resuspended into PBS. The conjugates were characterised using spectrometry, with a peak absorption at 532 nm.

2.3 Protein quantification
Conjugated protein was released from NPs using 0.1 mM mercaptoethanol (Sigma-Aldrich) which displaces the MHDA linker from the gold surface. The sample was then run through a 1 mm NuPAGE® 4-12% Bis-Tris gel at 180 V for 50 min, alongside known amounts of protein, before staining with Coomassie. The density of the resulting band was then compared against a concentration gradient to determine the amount of protein originally conjugated.

2.4 Immunisation

Groups of 5 female BALB/c mice, aged 6-8 weeks old were immunized by the intra-muscular (i.m.) route in 0.1 ml per mouse as follows: group 1 received 0.93 µg rF1-antigen conjugated NPs formulated in 0.26% w/v alhydrogel (AuNP-F1/alhy); group 2 received 0.93 µg rF1-antigen conjugated NPs in PBS (AuNP-F1/PBS); group 3 received empty nanoparticles in PBS (NP/PBS); group 4 received 0.93 µg rF1 formulated in 0.26% w/v alhydrogel (F1/alhy); and group 5 received 0.93 µg rF1 in PBS (F1/PBS). All groups were immunised on a single occasion only. The animals were closely observed following immunisation and were bled from the lateral tail vein each week to isolate sera for antibody analysis. The animals were euthanized after six weeks with terminal blood sampling and splenectomy.

2.5 Immunoanalysis

Sera from individual animals were assayed for F1- specific IgG titre by standard ELISA technique, as previously described (15). Briefly, serum samples were aliquoted to microtitre wells pre-coated in 5 µg/ml F1 (in PBS). Binding of serum was detected using an HRP-conjugated goat anti-mouse IgG (abcam; 1:5000 in 1% skimmed milk in TBS) followed by incubation (37$^{°}$C, 1 h). Plates were washed prior to the addition of ABTS substrate (Pierce) with subsequent reading of the absorbance at 415 nm. The relative concentrations of the isotypes IgG1 and IgG2a with F1 specificity were also determined by ELISA and a ratio of IgG1: IgG2a determined. Optical density was determined using a Multiskan plate reader and titres were determined by comparison with a standard curve on each ELISA plate, using Ascent software. Geometric mean titres were determined ± standard error of the mean for each treatment, allowing the statistical comparison of mean titres between treatment groups, using the Student's t-test.

The detection of antibody which competed for binding to F1 antigen *in vitro* with a protective macaque polyclonal antibody was determined as previously described (16). Briefly, rF1 antigen was coated (5 µg/ml) onto wells of a microtitre plate followed by binding of protective macaque sera. Individual serum samples were then added in duplicate in a 2-fold dilution starting with 1:100 in 1% (w/v) skimmed milk powder in TBS. Non-protective macaque sera was used as a negative control. The assay was developed with HRP-conjugated goat anti-mouse IgG (abcam; 1:5000 in 1% skimmed milk in TBS) followed by incubation (37$^{°}$C, 1 h). Plates were washed prior to the addition of ABTS substrate (Pierce) with subsequent reading of the absorbance at 415 nm.

2.6 Flow cytometric analysis

Spleens from individual mice were homogenised in Dulbecco's Modified Eagles Medium (DMEM) supplemented with L-glutamine, penicillin and streptomycin and the suspension of mixed splenocytes was washed by centrifugation (10,000 rpm; 5 min) prior to collecting the cell pellet and re-suspending the cells in DMEM supplemented as described above, with additional 10% v/v foetal calf serum. Live splenocytes were enumerated and 200 µl of each was aliquoted in duplicate to the wells of a 96-well plate, and rF1 was added to each well at a final concentration of

$25\mu g\ ml^{-1}$. Plates were incubated overnight ($37^{o}C$/ 5% CO2). Next day, plates were centrifuged to collect non-adherent cells and cell culture supernatants were collected and rapidly frozen ($-80^{o}C$) pending analysis of cytokines by cytometric bead assay (CBA, BD, UK). The non-adherent splenocytes were washed by centrifugation, collected and stained with a mastermix of antibodies specific for surface markers CD3, CD4, CD8 and CD45, and each labelled with a different chromophore (Becton-Dickenson, UK). Subsequently, antibody-bound cells were analysed by fluorescence activated cells sorting (FACS, Cantifluor, BD, UK) and the percentage and activation status of cells in the mixed splenocyte suspension was determined.

2.6 Statistical analysis
Student T-test was used to determine the significance of difference between treatment groups at the 95% confidence limit?.

3. Results

3.1 Preparation of gold nanoparticles
Synthesis of AuNPs followed the Turkevich method of gold chloride reduction using citrate ions, where the diameter of the particles is controlled by the concentration of the citrate. The particles then remain stable due to the repulsion of the anionic surface in the citrate solution. Characterisation of the particles using spectrometry showed them to be monodisperse with a λ_{max} of 519 nm (Fig. 1B). The particles were imaged using transmission electron microscopy (TEM) and shown to have a mean diameter of 15.6 nm, and the concentration measured using NP tracking analysis was $1.37\ x\ 10^{8}$ particles mL^{-1} (Fig. 1A).

3.2 Gold nanoparticle functionalisation
In order to conjugate F1-antigen onto the NPs a linker consisting of 16-mercaptohexadecanoic acid (MHDA) was first bound to the NP. The MHDA was covalently attached via a gold-sulphur bond, and formed a self-assembled monolayer (SAM) projecting a carboxyl group for linkage to the protein. Carboxylated NPs were purified from the bulk material, by centrifugation and washing, and then characterised by spectrophotometry, which revealed a shift in λ_{max} from 519 nm to 525 nm (Fig. 1B).

Carbodiimide coupling chemistry was used to conjugate the 15 kDa F1-antigen onto the MHDA linker. First, the concentration of F1-antigen required to saturate the NP surface was determined. Increasing concentrations of F1-antigen, in the range 0-50 μg/ml, were added to similar amounts of AuNPs. The binding of F1-antigen was assessed by monitoring the change in the wavelength of maximum absorption of visible light and also by the change in refractive index of the NPs (17). This revealed that the NPs were saturated when 30 μg/ml of F1-antigen was added (Fig. 2). The amount of protein conjugated onto the NPs was measured by purifying the nano-conjugates, using the centrifugation and wash method, and re-suspending into 2-mercaptoethanol. The alkanethiol solution displaced the thiol linker by competitively binding to the gold, releasing the F1-antigen. The released protein was analysed by 4-12% Bis-Tris gel stained with Coomassie blue, where the relative intensity of the

protein band could be quantified against a standard curve of known concentrations (Fig. 3). The amount of protein detected using this method was 0.3 µg of protein released from 10 µl NPs, equating to approximately 158 molecules per NP. Other proteins were also tethered onto AuNPs using this method including bovine serum albumin where 0.2 µg of protein was detected on a 4-12% Bis-Tris gel from a 10 µl sample. These findings suggest that loading is largely determined by steric (molecular weight), and compositional (lysine content) factors.

3.2 Immunisation study
To evaluate the immunogenicity of the F1-antigen AuNP conjugated vaccine, BALB/c mice were immunised intramuscularly with the purified nano-antigen with or without an aluminium hydroxide adjuvant (alhydrogel). The animals were observed for six weeks and the development of antibody to F1-antigen in sera was measured using an ELISA (Fig. 4). Control mice received F1-antigen in either alhydrogel or PBS, or AuNPs alone. After 14 days, mice given F1-antigen bound to NP in alhydrogel generated the greatest F1-antigen-specific antibody response (P < 0.01). This was followed by mice immunised with unbound F1-antigen in alhydrogel which generated a greater immune response than those in the groups with PBS instead of alhydrogel (P < 0.01). This suggests that it was not the addition of NPs alone that was generating a greater response but rather the combination of NPs with alhydrogel. Moreover there is a significant decline in IgG titres from mice immunised with unconjugated F1-antigen with or without alhydrogel from days 35 or 21 days respectively, post immunisation ($p < 0.01$). Mice given F1-antigen bound to NPs showed no decline in IgG titre at 42 days post-immunisation. Mice immunised with empty AuNPs alone did not develop antibody against F1-antigen (data not shown). Analysis of the IgG subclasses revealed that for all immunised groups, F1-specific IgG1 exceeded IgG2a (Table 1). However, the concentration of F1-specific IgG2a in mice immunised with AuNP-F1/PBS was significantly increased compared with mice administered unconjugated F1 in PBS ($p < 0.05$). Formulation of AuNP-F1/alhy significantly increased both IgG1 and IgG2a responses, ($p < 0.01$ and $p < 0.05$, respectively), compared with AuNP-F1/PBS.

Sera collected from individual treatment groups were assesed for their ability to compete with protective macaque antibody from rF1. In all cases, with the exception of AuNP, the mouse sera was able to displace the macaque sera over a series of dilutions. Sera from animals immunised with AuNP-F1/alhy competed most succesfully with the macaque antibody, with a significantly greater percentage bind than any other group for the intial two dilutions ($p < 0.01$). Whereas mice immunised with AuNP-F1 and unconjugated F1 competed with the macaque sera to the same degree, when immunised with the addition of alhydrogel the AuNP-F1/alhy group competed twice as well as those given F1/alhy.

3.3 Flow cytometric analysis
Flow cytometric analysis showed that a high percentage of cells positive for the activation/maturation marker CD45 existed in all treatment groups (Table 2). CD4+ cells as a percentage of cells bearing the pan T-cell marker (CD3) exceeded CD8+ cells as a percentage of the CD3+ population, for all treatment groups, with no

significant differences between groups. Analysis of IFNγ in the culture supernatant of splenocytes re-stimulated *ex vivo* with F1, revealed a significantly reduced level from cells obtained from mice immunised with AuNP-F1/alhy, compared with those from mice administered F1/PBS ($P < 0.05$), indicating the anti-inflammatory influence of alhydrogel in the vaccine formulation.

4. Discussion

Yersinia pestis is the causative agent of plague, a human disease which is associated with a high level of mortality (18). Although the bacterium no longer causes pandemics of disease, WHO estimates that there are approximately 3000 cases of plague annually world-wide, mainly in N. America, S. E. Asia and Africa (18). The F1-antigen is a major component of the surface of *Y. pestis* and forms a capsule-like structure which is visible after negative staining of bacteria (19).

Intramuscular immunisation with recombinant F1-antigen, purified from *E. coli* has previously been shown to induce a protective immune response against *Y. pestis* (15, 20, 21) and a subunit vaccine composed of *Y. pestis* F1-antigen and recombinant V antigen (a secreted *Y. pestis* protein) shows potential as a replacement for the current killed whole cell vaccine (15, 22). However, alternative delivery systems which would permit either a simplified immunisation regimen (fewer doses) or a more appropriate immune response for protection (a balanced T_h1/T_h2 response with the establishment of cellular memory) are desirable.

We have used carbodiimide chemistry to link the F1-antigen to a MHDA linker which had first been immobilised onto the surface of the AuNP. We found this one-step conjugation to be a quick and reliable method for conjugating the F1-antigen, in contrast to electrostatic binding or maleimide chemistry, without modifying the protein. By ensuring that a non-ionic detergent, such as Triton X-100, was present during the conjugation process, we were able to separate NP-bound and free F1-antigen by centrifugation, avoiding inefficient gel chromatography steps. With the inclusion of Triton X-100, the particles were far more stable in close proximity to each other once pelleted and could be resuspended with ease. This method may be useful to other workers aiming to generate gold nanoconjugate vaccines.

The presentation of F1-antigen on the surface of AuNPs induced antibody responses which were superior to the responses induced by F1-antigen alone. NP conjugated F1 also generated higher IgG2a titres which would suggest activation of T_h1 cells however when IFNγ was measured there was a significant decrease in output from AuNP-F1/alhy compared to F1/PBS. Since AuNP-F1/PBS had a similarly high IFNγ output as F1/PBS this indicates that IFNγ is being supressed by the presence of alhydrogel. Previous work has shown that immunisation with multimers of F1-antigen provides enhanced protective immunity (13) and attenuated *Salmonella Typhimurium???* expressing F1-antigen on their surface are potent immunogens (19). Therefore, it is possible that the enhanced responses we have seen reflect the ability of NPs to present F1-antigen on their surface in a form which is similar to that on the surface of the bacterial cells. How about some mention of surface density?

Additionally, the nano-particulate nature of the AuNPs renders them strongly immunogenic and readily taken up by macrophages for presentation to T-cells to induce cell-mediated immunity.

We have not tested whether mice immunised with F1-antigen on AuNPs are protected against an experimental *Y. pestis* challenge. However, when compared with protective sera isolated from macaques, AuNP-F1/alhy competed for the same F1 epitopes displacing the macaque sera. This suggests that the mouse sera is functional and raised against the same epitopes as the macaque sera. The antibody levels we have measured in immunised mice and their ability to displace protective macaque sera indicate that the immunised mice would be protected against *Y. pestis* infection.

There have also been numerous studies, including those listed, have shown that antibody and appropriate CMI is important in protection against plague (23-26). This is in accordance with the intracellular lifestyle of *Y. pestis.* Immunisation of mice with the plague sub-unit (F1 and V antigens) vaccine resulted in a strong total IgG1 response, which correlated with protection (25, 27). Furthermore, transfer of mouse hyperimmune serum into naïve mice protected them against plague challenge (25, 27).

Previously, polylactide microspheres have been used to encapsulate F1-antigen, and immunisation with these microspheres resulted in the induction of protective immuntiy against a *Y. pestis* challenge (15). However, the authors noted that the response was slow to develop, which they atrributed to the slow release of antigen from the polylactide microspheres; something which is true of many encapsulation strategies (28-30). The AuNPs we have used in this study are easily prepared in the laboratory and the data we report here indicates there was no delay in the induction of protective immunity. This observation suggests that the F1-antigen is not released from the surface of the NP after dosing. Rather, it seems likely that each NP is taken up and processed by antigen presenting cells.

A wide variety of NP delivery systems have been proposed including polymeric NPs, solid lipid NPs, nanostructured lipid carriers, dendrimers, cyclodextrins, fullerenes, gold and silica NPs, and quantum dots. Some of these, including AuNPs, are being assessed as drug delivery systems (31-37). More recently there has been interest in the use use of AuNPs to deliver protein vaccine antigens.

Previous workers have shown that the size of the AuNP used to deliver vaccines can have a profound influence on uptake into mamalian cells and on the antibody response (38-40). Although responses to a Foot and Mouth Disease Virus peptide were observed using 2-17nm AuNP carriers, the optimal response was elicited using 8nm AuNPs. Peptides linked to larger (37 or 50nm) AuNPs failed to elicit antibody responses. Like us, other workers have used 15nm AuNPs as the carrier for merozoite surface protein 1 (41) or Nogo-66 receptor (42) to elicit antibody responses.

Other workers (38, 41, 42) have reported the ability of AuNPs to enhance the ability of antigen to evoke antibody responses compated with antigen given alone. In the case of merozoite surface protein 1 or Nogo-66 receptor the use of AuNPs as a delivery vehicle resulted in the induction of antibody responses exceeding those elicited by the antigen given with Freunds adjuvant (41, 42). Some workers have reported that the use of alum as an adjuvant further enhanced the responses elicited by antigen bound to AuNPs (41) but others have used antigen bound to AuNPs without an additional adjuvant (38, 42). Similarly we also found in our study that the use of alum as an adjuvant to antigen linked to AuNPs enhanced the antibody response to F1-antigen.

Whilst our results are encouraging, the utility of NPs as vaccine carriers requires significant additional investigation. Although gold has been used widely in medicine, there are some recent publications that suggest AuNPs can accumulate within tissues and elicit toxic effects *in vivo* (10, 43). These recent reports of toxicity involve studies where high doses of NPs are repeatedly given intraperitoneally. Clearly, toxicity may not be a concern when single doses of NPs are given intramuscularly and there is also literature to suggest that there is no evidence of toxicity associated with AuNPs (42, 44).

In addition, further work is required to determine the fate of AuNPs given intramuscularly and, the mechanisms by which AuNPs are taken up into antigen presenting cells require clarification. Our results show that the ratio of serum IgG1 to IgG2a was similar in mice that had been dosed with free F1-antigen or F1-antigen coupled to AuNPs. This finding suggests that both antigens are taken up by a similar pathway into antigen presenting cells.

In conclusion our findings add to the growing body of evidence showing that the use of AuNPs as carriers can markedly enhance the ability of protein antigens to elicit antibody responses.
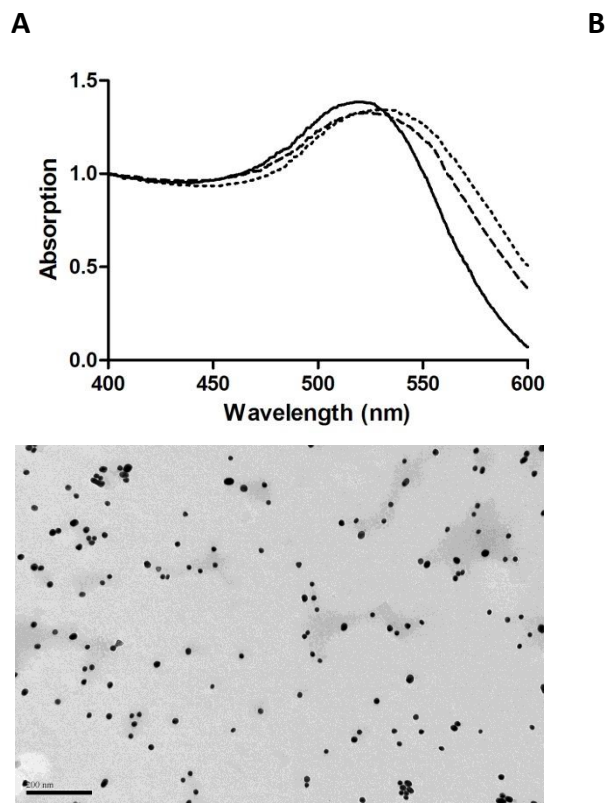
A   **B**

Figure 1. Characterisation of AuNPs (A) Optical extinction- yes this is the right word but the graph is labelled as absorbance profile of gold nanoparticles using a UV-visible spectrophotometer. λ max for AuNP is 519nm (solid), carboxylated AuNP is 525nm (dashed) and F1 conjugated AuNP is 532nm (dotted). **(B)** Image of gold nanoparticles taken with a Jeol JEM-1400 transmission electron microscope measured average diameter of 15.6 nm.
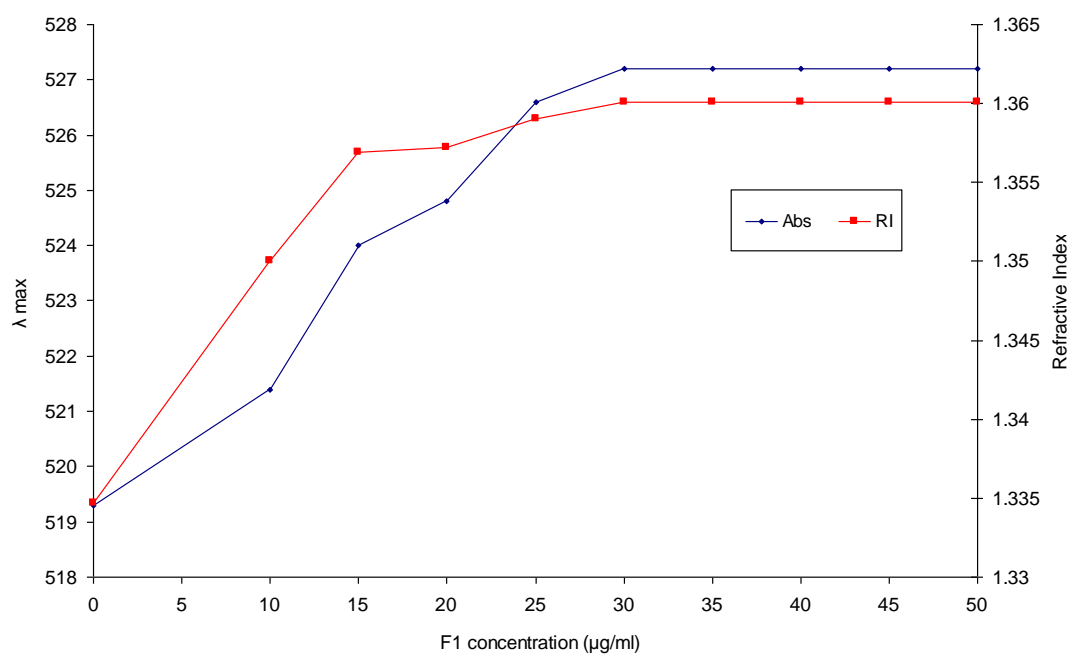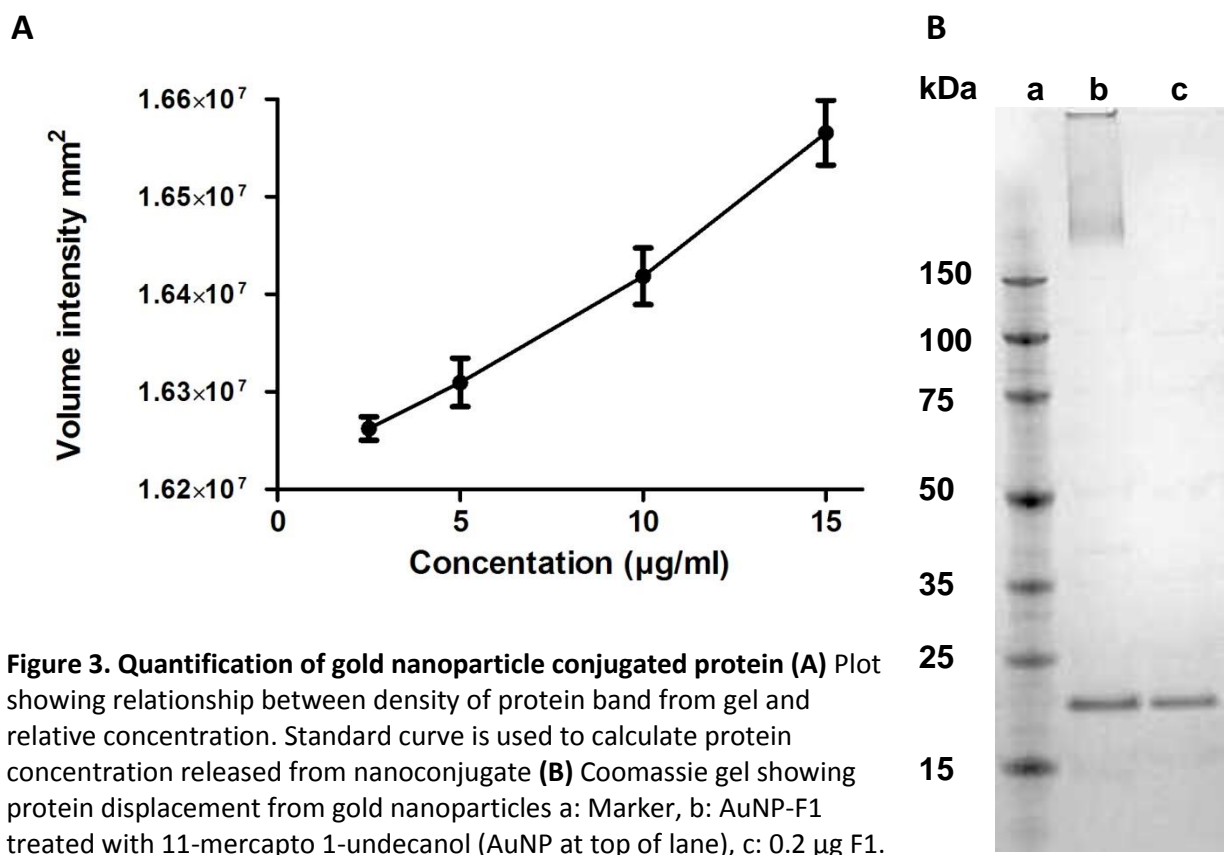
FIGURE 2 Minimum protein concentrations required for AuNP saturation can be concluded from measuring λ_{max} over a range of F1-antigen concentrations. Graph shows a representative data set from three replicates. All measurements were made using a UV-visible spectrophotometer to 0.1 nm.
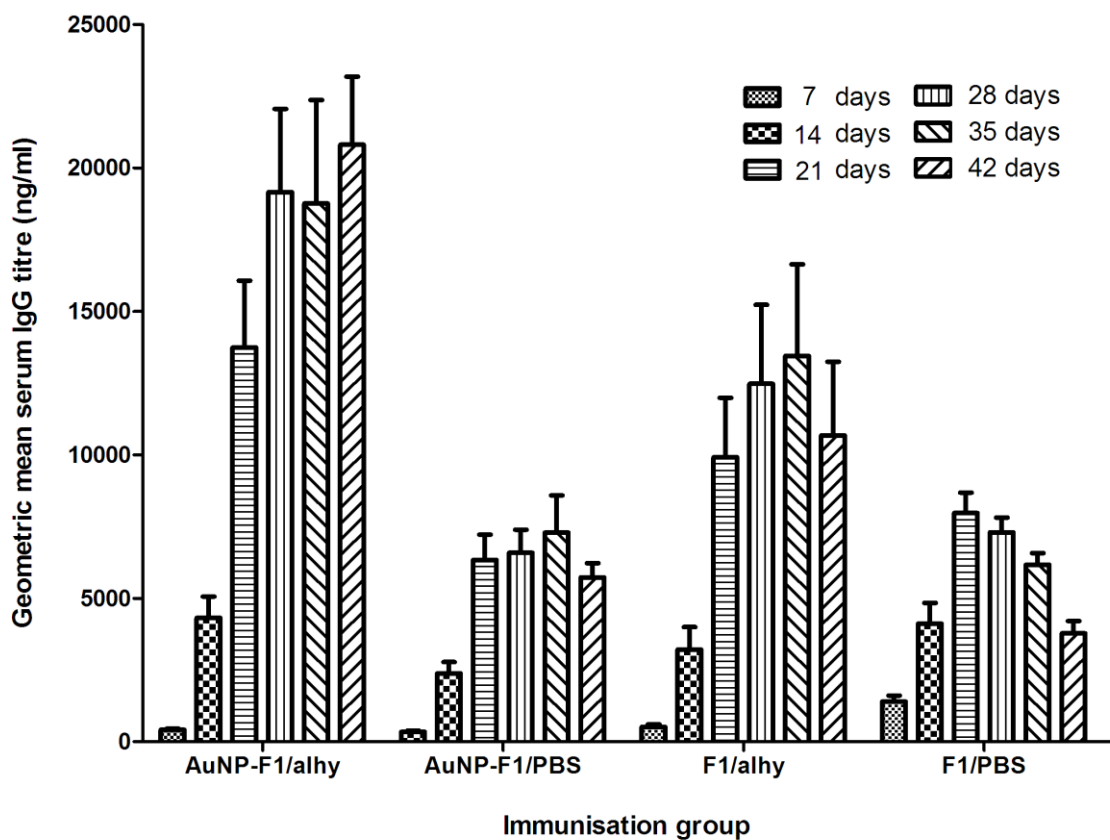
A

B

Figure 3. Quantification of gold nanoparticle conjugated protein (A) Plot showing relationship between density of protein band from gel and relative concentration. Standard curve is used to calculate protein concentration released from nanoconjugate **(B)** Coomassie gel showing protein displacement from gold nanoparticles a: Marker, b: AuNP-F1 treated with 11-mercapto 1-undecanol (AuNP at top of lane), c: 0.2 μg F1.

Figure 4. Relative concentrations of F1-specific total IgG in sera from BALB/c mice. After 14 days, mice immunised with gold nanoparticle -conjugated F 1 in alhydrogel generated a significantly higher IgG titre compared with gold nanoparticle -conjugated F 1 in PBS and unconjugated F1 in PBS ($P < 0.01$). Gold nanoparticle – conjugated F1 in alhydrogel mice were the only ones not to show a decline in total IgG at 42 days post-immunisation. Each point is the mean of values from five mice

Antigen	IgG1 (µg/ml)	IgG2a (µg/ml)	Ratio IgG1:IgG2a
AuNP-F1/alhy	22.95±3.83	1.67±0.11	13.75
AuNP-F1/PBS	6.59±0.86	0.98±0.13	6.72
F1/alhy	12.53±3.15	0.86±0.18	14.57
F1/PBS	6.46±0.39	0.46±0.07	14.04

Table 1. Analysis of F1-specific IgG1 and IgG2a isotypes in sera taken from immunised mice. The concentration of F1-specific IgG2a in mice immunised with gold nanoparticle - conjugated F 1 in PBS was significantly increased compared with mice administered unconjugated F1 in PBS ($p<0.05$). Formulation of F1-conjugated gold nanoparticles in alhydrogel significantly increased both IgG1 and IgG2a responses, ($p<0.01$ and $p<0.05$, respectively), compared with F1-conjugated gold nanoparticles in PBS.
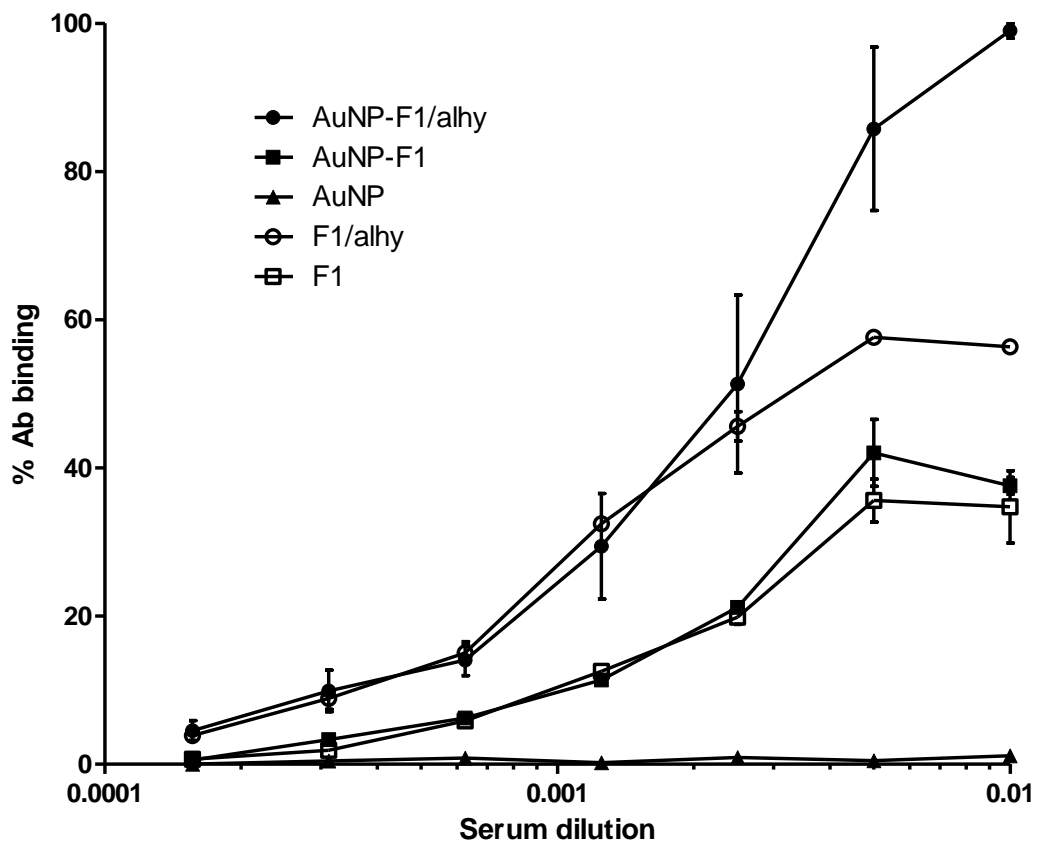
Figure 5. Competitive ELISA for binding to F1. After 14 days, mice immunised with gold nanoparticle -conjugated F 1 in alhydrogel generated a significantly higher IgG titre compared with gold nanoparticle -conjugated F 1 in PBS and unconjugated F1 in PBS (P < 0.01). Gold nanoparticle – conjugated F1 in alhydrogel mice were the only ones not to show a decline in total IgG at 42 days post-immunisation. Each point is the mean of values from five mice

Group	CD45+ (% of CD3+ cells ± s.e.m.) specifically activated by F1 *ex vivo*	IFNγ output (ng/ml ± s.e.m.) in recall response specific for F1
AuNP-F1/alhy	89.8±2.2	327±24
AuNP-F1/PBS	86.0±5.0	704±187
F1/alhy	82.04±10.3	542±121
F1/PBS	74.8±14	775±113

Table 2. Percentage of CD3+ splenocytes displaying the activation marker CD45 *on ex vivo* re-stimulation with rF1. For all treatment groups, CD3$^+$CD4$^+$ cells outnumbered CD3$^+$CD8$^+$ cells by approximately 2:1, with no significant differences between groups. The secretion of IFNγ by restimulated splenocytes was significantly reduced in the group receiving AuNP-F1/alhydrogel, compared with the F1/PBS group ($p < 0.05$).

5. References

1. Evans RG, Crutcher JM, Shadel B, Clements B, & Bronze MS (2002) Terrorism from a public health perspective. *Am J Med Sci* 323(6):291-298.
2. Fahmy TM, Fong PM, Park J, Constable T, & Saltzman WM (2007) Nanosystems for simultaneous imaging and drug delivery to T cells. *Aaps J* 9(2):E171-180.
3. Bi R & Zhang N (2007) Liposomes as a Carrier for Pulmonary Delivery of Peptides and Proteins. *Journal of Biomedical Nanotechnology* 3(4):332-341.
4. Cryan SA (2005) Carrier-based strategies for targeting protein and peptide drugs to the lungs. *Aaps J* 7(1):E20-41.
5. Anabousi S*, et al.* (2006) Effect of PEGylation on the Stability of Liposomes During Nebulisation and in Lung Surfactant. *Journal of Nanoscience and Nanotechnology* 6(9-10):3010-3016.
6. Bawarski WE, Chidlowsky E, Bharali DJ, & Mousa SA (2008) Emerging nanopharmaceuticals. *Nanomedicine: Nanotechnology, Biology, and Medicine* 4:273–282.
7. Matsumura Y & Maeda H (1986) A new concept for macromolecular therapeutics in cancer chemotherapy: mechanism of tumoritropic accumulation of proteins and the antitumor agent smancs. *Cancer Res* 46(12 Pt 1):6387-6392.
8. Pissuwan D, Cortie CH, Valenzuela SM, & Cortie MB (2007) Gold Nanosphere-Antibody Conjugates for Hyperthermal Therapeutic Applications. *Gold Bulletin* 40:121-129.
9. Yamamoto A, Honma R, Sumita M, & Hanawa T (2003) Cytotoxicity evaluation of ceramic particles of different sizes and shapes. *Journal of biomedical meaterials research part A* 68A(2):244-256.
10. Lasagna-Reeves C*, et al.* (2010) Bioaccumulation and toxicity of gold nanoparticles after repeated administration in mice. *Biochem Biophys Res Commun* 393(4):649-655.
11. Lovric J, Cho SJ, Winnik FM, & Maysinger D (2005) Unmodified Cadmium Telluride Quantum Dots Induce Reactive Oxygen Species Formation Leading to Multiple Organelle Damage and Cell Death. *Chemistry & Biology* 12(11):1227-1234.
12. Chen D, Zhang D, Yu JC, & Chan KM (2011) Effects of Cu2O nanoparticle and CuCl2 on zebrafish larvae and a liver cell-line. *Aquat Toxicol* 105(3-4):344-354.
13. Miller J*, et al.* (1998) Macromolecular organisation of recombinant Yersinia pestis F1 antigen and the effect of structure on immunogenicity. *FEMS Immunol Med Microbiol* 21(3):213-221.
14. Turkevich J, Stevenson PC, & Hillier J (1951) A study of the nucleation and growth processes in the synthesis of colloidal gold. *Discuss. Faraday Soc.* 11:55-75.
15. Williamson DE*, et al.* (1996) Local and systemic immune response a microencapsulated sub-unit vaccine to for plague. *Vaccine* 14:1613-1619.
16. Williamson ED*, et al.* (2005) Human Immune Response to a Plague Vaccine Comprising Recombinant F1 and V Antigens. *Infect. Immun.* 73:3598–3608.

17. Brewer SH, Glomm WR, Johnson MC, Knag MK, & Franzen S (2005) Probing BSA Binding to Citrate-Coated Gold Nanoparticles and Surfaces. *Langmuir* 21:9303-9307.

18. Perry RD & Fetherston JD (1997) *Yersinia pestis*—Etiologic Agent of Plague. *Clinical Microbiology Reviews* 10:35-66.

19. Titball RW, Howells AM, Oyston PC, & Williamson ED (1997) Expression of the *Yersinia pestis* capsular antigen (F1 antigen) on the surface of an aroA mutant of *Salmonella typhimurium* induces high levels of protection against plague. *Infect Immun* 65(5):1926-1930.

20. Simpson WJ, Thomas RE, & Schwan TG (1990) Recombinant capsular antigen (fraction 1) from *Yersinia pestis* induces a protective antibody response in BALB/c mice. *Am J Trop Med Hyg* 43(4):389-396.

21. Andrews GP, Heath DG, Anderson GW, Jr., Welkos SL, & Friedlander AM (1996) Fraction 1 capsular antigen (F1) purification from *Yersinia pestis* CO92 and from an *Escherichia coli* recombinant strain and efficacy against lethal plague challenge. *Infect Immun* 64(6):2180-2187.

22. Quenee LE, Ciletti NA, Elli D, Hermanas TM, & Schneewind O (2011) Prevention of pneumonic plague in mice, rats, guinea pigs and non-human primates with clinical grade rV10, rV10-2 or F1-V vaccines. *Vaccine* 29(38):6572-6583.

23. Shepherd AJ, Hummitzsch DE, Leman PA, Swanepoel R, & Searle LA (1986) Comparative tests for detection of plague antigen and antibody in experimentally infected wild rodents. *Journal of Clinical Microbiology* 24(6):1075-1078.

24. Williams JE, Arntzen L, Tyndal GL, & Isaacson M (1986) Application of enzyme immunoassays for the confirmation of clinically suspect plague in Namibia. *Bull. World Health Organ.* 64(5):745-752.

25. Williamson ED*, et al.* (1999) An IgG1 titre to the F1 and V antigens correlates with protection against plague in the mouse model. *Clin. Exp. Immunol.* 116(1):107-114.

26. Quenee LE & Schneewind O (2009) Plague vaccines and the molecular basis of immunity against *Yersinia pestis*. *Hum. Vaccines* 5(12):817-823.

27. Williamson ED*, et al.* (1997) A sub-unit vaccine elicits IgG in serum, spleen cell cultures and bronchial washings and protects immunized animals against pneumonic plague. *Vaccine* 15(10):1079-1084.

28. Alonso MaJ, Gupta RK, Min C, Siber GR, & Langer R (1994) Biodegradable microspheres as controlled-release tetanus toxoid delivery systems. *Vaccine* 12(4):299-306.

29. O'Hagan DT, Jeffery H, Roberts MJJ, McGee JP, & Davis SS (1991) Controlled release microparticles for vaccine development. *Vaccine* 9(10):768-771.

30. Alonso MJ*, et al.* (1993) Determinants of Release Rate of Tetanus Vaccine from Polyester Microspheres. *Pharmaceutical Research* 10(7).

31. Paciotti GF*, et al.* (2004) Colloidal Gold: A Novel Nanoparticle Vector for Tumor Directed Drug Delivery. *Drug Delivery* 11(3):169-183.

32. Soppimath KS, Aminabhavi TM, Kulkarni AR, & Rudzinski WE (2001) Biodegradable polymeric nanoparticles as drug delivery devices. *Journal of Controlled Release* 70(1-2):1-20.

33.   Hans ML & Lowman AM (2002) Biodegradable nanoparticles for drug delivery and targeting. *Current Opinion in Solid State and Materials Science* 6(4):319-327.

34.   Davis ME (2009) The First Targeted Delivery of siRNA in Humans via a Self-Assembling, Cyclodextrin Polymer-Based Nanoparticle: From Concept to Clinic. *Molecular Pharmaceutics* 6(3):659-668.

35.   Ruan G, Agrawal A, Marcus AI, & Nie S (2007) Imaging and Tracking of Tat Peptide-Conjugated Quantum Dots in Living Cells: New Insights into Nanoparticle Uptake, Intracellular Transport, and Vesicle Shedding. *Journal of the American Chemical Society* 129(47):14759-14766.

36.   Derfus AM, Chen AA, Min D-H, Ruoslahti E, & Bhatia SN (2007) Targeted Quantum Dot Conjugates for siRNA Delivery. *Bioconjugate Chemistry* 18(5):1391-1396.

37.   Trewyn BG, Giri S, Slowing II, & Lin VSY (2007) Mesoporous silica nanoparticle based controlled release, drug delivery, and biosensor systems. *Chemical Communications* (31):3236-3245.

38.   Chen YS, Hung YC, Lin WH, & Huang GS (2010) Assessment of gold nanoparticles as a size-dependent vaccine carrier for enhancing the antibody response against synthetic foot-and-mouth disease virus peptide. *Nanotechnology* 21(19):195101.

39.   Chithrani BD, Ghazani AA, & Chan WCW (2006) Determining the Size and Shape Dependence of Gold Nanoparticle Uptake into Mammalian Cells. *Nano Letters* 6(4):662-668.

40.   Yue H*, et al.* (2010) Particle size affects the cellular response in macrophages. *Eur J Pharm Sci* 41(5):650-657.

41.   Parween S, Gupta PK, & Chauhan VS (2011) Induction of humoral immune response against PfMSP-1(19) and PvMSP-1(19) using gold nanoparticles along with alum. *Vaccine* 29(13):2451-2460.

42.   Wang Y-T*, et al.* (2011) The use of a gold nanoparticle-based adjuvant to improve the therapeutic efficacy of hNgR-Fc protein immunization in spinal cord-injured rats. *Biomaterials* 32(31):7988-7998.

43.   Abdelhalim MAK & Mady MM (2011) Liver uptake of gold nanoparticles after intraperitoneal administration in vivo: A fluorescence study. *Lipids Health Dis.* 10:9.

44.   Connor EE, Mwamuka J, Gole A, Murphy CJ, & Wyatt MD (2005) Gold nanoparticles are taken up by human cells but do not cause acute cytotoxicity. *Small* 1:325-327.